AD-A231 651

USAFETAC/PR-90/005

2

EFFECTIVE SUNSPOT NUMBER (SSNi) COMPARISON STUDY

by

Capt Mary L. Hart

DECEMBER 1990

USAF
ENVIRONMENTAL TECHNICAL
APPLICATIONS CENTER

Scott Air Force Base, Illinois, 62225-5438

REVIEW AND APPROVAL STATEMENT

USAFETAC/PR-90/005, *Effective Sunspot Number (SSNi) Comparison Study*, December 1990, has been reviewed and is approved for public release. There is no objection to unlimited distribution of this document to the public at large, or by the Defense Technical Information Center (DTIC) to the National Technical Information Service (NTIS).

Patrick J. Breitling

PATRICK J. BREITLING
Chief Scientist

FOR THE COMMANDER

Walter S. Burgmann

WALTER S. BURGMANN
Scientific and Technical Information
Program Manager
21 December 1990

REPORT DOCUMENTATION PAGE

2. Report Date: December 1990

3. Report Type: Project Report

4. Title and Subtitle: Effective Sunspot Number (SSNi) Comparison Study

6. Author: Capt Mary L. Hart

7. Performing Organization Name and Address: USAF Environmental Technical Applications Center (USAFETAC/DNE), Scott AFB, IL 62225-5438

8. Performing Organization Report Number: USAFETAC/PR-90/005

12. Distribution/Availability Statement: Approved for public release; distribution is unlimited.

13. Abstract: Report documents the results of a USAFETAC study done to determine whether or not reliable global Effective Sunspot Numbers (SSNis) for the Air Force Global Weather Central's (AFGWC's) Ionospheric Conductivity and Electron Density (ICED) model could be calculated based on the present number (11) of digital ionosonde sites. The study found that increasing the number of sites would have a limited effect on ICED output, and that it was feasible to run the ICED model using the present 11-station network, subject to certain limitations.

14. Subject Terms: SOLAR ACTIVITY, SOLAR DISTURBANCES, SUNSPOTS, ELECTRON DENSITY, IONOSONDES, IONOSPHERIC MODELS, AIR FORCE GLOBAL WEATHER CENTRAL

15: Number of Pages: 39

17. Security Classification of Report: Unclassified

18. Security Classification of this Page: Unclassified

19. Security Classification of Abstract: Unclassified

20. Limitation of Abstract: UL

Standard Form 298

PREFACE

This report documents the results of a study done for AFGWC/WSE as USAFETAC Project 900919. The analyst was Capt Mary L. Hart, USAFETAC/DNE. The purpose was to determine whether or not reliable global Effective Sunspot Numbers (SSNis) for AFGWC's Ionospheric Conductivity and Electron Density (ICED) model could be calculated based on the present limited number (11) of ionosonde sites. AFGWC needed the results of this study to decide whether or not their current ionosonde data network could be used to generate SSNis, or if additional Digital Ionospheric Sounding System (DISS) sites would have to be added to the network. The study found that increasing the number of ionosonde stations would have a limited effect on the output of today's highly climatological ICED model. It was concluded that it was feasible to run today's ICED model using the present 11-station near-real time ionosonde network, subject to certain limitations described herein. Because ICED is not the model Air Weather Service plans to use for future ionospheric support, it is not valid to use the conclusions of this study for determining the density of future ionospheric networks like DISS.

CONTENTS

FIGURES

TABLES

EFFECTIVE SUNSPOT NUMBER (SSNI) COMPARISON STUDY

1. INTRODUCTION

1.1 Purpose. The purpose of this study was to determine whether or not reliable global Effective Sunspot Numbers (SSNis) for AFGWC's Ionospheric Conductivity and Electron Density (ICED) model can be calculated based on a limited number of ionsonde sites. Although AFGWC/WSE needs near-real time SSNis for ICED, it receives such data from only 11 ionosonde sites. AFGWC needed the results of this study to decide whether or not their current ionosonde data network could be used to generate SSNis.

1.2 The Quality Control Program. The ICED Model uses an effective sunspot number (SSNi) as an input. Mr Herb Kroehl (National Geophysical Data Center--NGDC) developed a method for calculating SSNis from ionosonde data using the critical frequency of the F2 layer (foF2). He provided AWS with two FORTRAN programs that partially automate the calculation process. The first program (QC) reads a file of hourly foF2 data for a single ionosonde site for a specified month. The program uses the first day of the month as a reference day and does a day-by-day comparison of foF2's for the month. Every hourly foF2 that differs from the reference value by a certain percentage (25 percent during the day, 50 percent at night) is flagged for manual check by an analyst. QC also checks the daylight hours (06-18 local) for significant variations in foF2 that signal storm activity. When ionospheric storms occur during daylight hours, heating and transport effects in the upper atmosphere cause electron loss in the F2 layer of the ionosphere that will tend to reduce observed foF2s. When more than half the daylight hours differ from the reference hours by more than 25 percent, QC flags that day as a storm day.

1.3 The SSNE Program. After the analyst checks flagged foF2s manually, the second program (SSNE) calculates SSNis from the "clean" foF2 data. SSNis are calculated from ionosonde data, using multiple ionosonde site data as input. The number of sites used is determined by the size of the geographical area the SSNis are meant to represent. When global SSNis are calculated, between 35 and 40 sites are commonly used. When calculating SSNis, the analyst also specifies the period of record (POR--in this case, usually a month), the geographical area, and the associated weighting factors (two temporal and four latitudinal factors). An foF2 weighting factor for each ionosonde site is also needed. SSNE outputs hourly SSNis for each day of the POR. The SSNis are effective sunspot numbers developed specifically for use as input to ICED.

2. DATA.

2.1 Hourly foF2 Data. Hourly foF2 data from the USAFETAC Space Environmental Support System (SESS) Climatic Database (SCDB) for 36 ionosonde sites specified by AFGWC/WSE were used in this study. Period of record (POR) was from 1 February to 31 July 1990. Table 1 lists the 36 stations used to provide the control group of SSNis for this study. The 11 stations used to calculate the test SSNis, a subset of this group, are identified in the table by underlining. Some locations in the 11-station subset (such as Resolute Bay, Akita, Wakkanai, and Okinawa) are not full-time reporting stations. Others in the subset (such as Cape Canaveral and Bermuda) have a fairly high number of questionable observations. The effects that foF2 data quality had on the results will be discussed in Section 4, "Limitations."

2.2 Equivalent Auroral Index. Another ICED input, the equivalent auroral index (Qe), also came from the USAFETAC SCDB. Because the Qe values needed by ICED were not present in the SCDB for every hour of the POR, the analyst calculated a mean daily Qe for the POR. This was used with the control and test SSNis as model input.

TABLE 1. Global Set of Ionosonde Sites. Stations in the 11-station subset used as the test group are underlined.

Krenkel	(80.6° N, 58.1° E)	Nicosia	(35.2° N, 33.3° E)
Dixon	(73.5° N, 80.4° E)	Bermuda	(32.5° N, 64.7° W)
Murmansk	(69.0° N, 33.0° E)	Wakkanai	(45.5° N, 141.61° E)
Salekhard	(66.5° N, 66.7° E)	Boulder	(40.0° N, 105.3° W)
Uppsala	(59.8° N, 17.6° E)	Goose Bay	(54.3° N, 60.3° W)
Resolute Bay	(74.7° N, 94.9° W)	Vandenberg	(34.7° N, 120.6° W)
Sverdlovsk	(56.7° N, 61.1° E)	Akita	(39.8° N, 140.1° E)
Tomsk	(56.5° N, 84.9° E)	Ottawa	(45.4° N, 75.9° W)
St Peter	(54.2° N, 8.4° E)	Khabarovsk	(48.5° N, 135.1° E)
College	(64.9° N, 147.8° W)	Irkutsk	(52.5° N, 104.0° E)
Kiev	(50.7° N, 30.3° E)	Argentia	(47.31° N, 54.0° W)
Poitiers	(46.6° N, 0.4° E)	Wallops Is	(37.9° N, 75.5° W)
Cape Schmidt	(68.9° N, 179.5° W)	Okinawa	(26.3° N, 127.8° E)
Churchill	(58.8° N, 94.2° W)	Cape Canaveral	(28.5° N, 80.6° W)
Slough	(51.5° N, 0.6° W)	Kahului	(20.8° N, 156.5° W)
Ashkhabad	(38.0° N, 58.2° E)	Taipei	(25.0° N, 121.2° E)
Magadan	(60.0° N, 151.0° E)	Manila	(14.6° N, 121.0° E)
Yakutsk	(62.0° N, 129.6° E)	Camden	(34.0° S, 150.6° E)

3. METHODOLOGY.

3.1 Quality Control. The analyst QC'ed foF2 data for the 36 ionosonde sites shown in Table 1, using the process developed by NGDC. The SSNE program was used to calculate two sets of hourly SSNis (using the 36-station control and the 11 station subset data) for each day of the POR (by month). SSNi and Qe values were used as input to a modified version of ICED. This version of ICED calculates and outputs a series of hourly foF2s for a single location over a specified POR; it was validated against test data from AFGWC during a prior USAFETAC Project (900022601). AFGWC requested that ICED be run for six locations (Vandenberg, Sverdlovsk, Ashkabad, Cape Canaveral, Slough, and Magadan), and that the model foF2s for the control and test groups be compared to foF2s observed during the POR. Storm days for each of the six locations were determined by the QC program using the criteria discussed in 1.2. A census of foF2 observations available from each of the six stations shown in Table 2 shows the number of quiet cases, storm cases, and all cases reported for each hour during the POR. The census showed that there were substantial gaps in the SCDB, and that some stations have almost no storm cases.

TABLE 2. Observed foF2 Counts in SCDB (POR: 1 Feb-31 Jul 1990).

	Vandenberg			Sverdlovsk			Ashkhabad		
Hr(Z)	*Quiet*	*Storm*	*All*	*Quiet*	*Storm*	*All*	*Quiet*	*Storm*	*All*
00	139	33	172	126	18	144	135	4	139
01	138	33	171	127	19	146	154	3	157
02	138	34	172	125	21	151	148	4	152
03	134	31	165	126	25	151	140	3	143
04	139	31	170	123	22	145	131	1	132
05	134	32	166	123	20	143	127	3	130
06	132	31	163	118	16	134	126	2	128
07	136	31	167	130	27	157	137	2	139
08	132	31	163	126	22	148	138	4	142
09	136	33	169	122	22	144	139	4	143
10	137	33	170	119	23	142	137	2	139
11	135	33	168	125	20	145	119	3	122
12	132	34	166	112	20	132	133	3	136
13	132	35	167	122	21	143	130	3	133
14	135	32	167	114	22	136	114	2	116
15	140	33	173	125	23	148	116	4	120
16	140	32	172	127	23	150	97	3	100
17	141	35	176	127	22	149	94	3	97
18	140	35	175	123	18	141	98	3	101
19	136	32	168	125	20	145	122	3	125
20	138	33	171	131	18	149	123	5	128
21	134	33	167	130	19	149	126	5	131
22	134	35	169	128	18	146	131	4	135
23	138	35	173	127	18	145	130	5	135
Total	*3270*	*790*	*4060**	*2981*	*497*	*3478**	*3045*	*78*	*3123**

TABLE 2. Observed foF2 Counts in SCDB (POR: 1 Feb-31 Jul 1990), Cont'd.

	Cape Canaveral			Slough			Magadan		
Hr(Z)	*Quiet*	*Storm*	*All*	*Quiet*	*Storm*	*All*	*Quiet*	*Storm*	*All*
00	49	11	60	132	12	144	114	14	128
01	42	3	45	131	13	144	120	14	134
02	51	8	59	130	23	153	114	15	129
03	76	7	83	129	13	142	111	19	130
04	76	9	85	129	14	143	105	16	121
05	99	8	107	129	15	144	106	18	124
06	93	7	100	135	16	151	115	24	139
07	115	15	130	135	16	151	114	27	141
08	124	16	140	134	16	150	124	26	150
09	105	13	118	135	15	150	124	28	152
10	101	6	107	135	13	148	117	24	141
11	48	6	54	137	15	152	112	25	137
12	70	11	81	137	15	152	105	21	126
13	86	13	99	137	14	151	101	15	116
14	102	16	118	137	14	151	83	15	98
15	101	8	109	136	14	150	81	13	94
16	99	7	106	136	15	151	83	19	102
17	101	10	120	134	15	149	83	17	100
18	88	12	100	136	15	151	100	17	117
19	92	10	102	137	15	152	100	19	119
20	92	14	106	131	14	145	105	21	126
21	97	13	110	127	15	142	105	26	131
22	104	14	118	133	15	148	112	25	137
23	82	13	95	131	15	146	108	23	131
Total	*2093*	*250*	*2343**	*3203*	*347*	*3550**	*2543*	*481*	*3024**

*Note: If there were no missing observations, each station would have a total of 4,344 foF2 values.

3.2 Calculations. The mean, standard deviation, skewness, and median difference between modeled and observed foF2, and the correlation and RMS error between modeled and observed foF2, were then calculated for the six stations in Table 2. These statistics were calculated for the following categories: the entire POR, the quiet days of the POR, and the storm days of the POR. The normality of each difference distribution was determined by a skewness test. The skewness of each distribution was compared to the standard deviation of a normal population of the same size, where the standard deviation equals the square root of 6 divided by the number of observations. If the skewness is greater than three times the standard deviation, the null hypothesis of normality is rejected. If the skewness is less than three times the standard deviation, the distribution may be normal and the assumptions of normality can be used.

4. LIMITATIONS.

4.1 Short Period of Record, Missing Observations. The main limitations in this study were the short POR and the small amount of data available due to missing observations. USAFETAC had ionosonde data covering a much larger POR, but the amount of man hours needed to extract the data, QC it, and run it through ICED made it impossible to meet the quick response required by AFGWC/WSE. The limitations imposed by the smaller POR were acceptable to AFGWC/WSE. Because the short POR contains mostly 1990 summer data, it won't show the effect of seasonal or solar cycle variation in foF2 on model results. Although 1990 was near the peak of the solar cycle, the relative lack of large flares and subsequent storms means that the model results are somewhat better than would be the case if the POR had contained more storm days. The small POR and lack of storm days means that most of the six study sites in Table 2 have too small a storm sample size to provide any significant results, especially when the sample is subdivided into hourly results. A sample size of at least 30 storm days (720 hourly observations) out of a 181-day POR is large enough to ensure that there is a low probability of the results being unduly influenced by a few extreme data values. The only station with enough storm days to compute statistics from the hourly values was Vandenberg.

4.2 foF2 Data Quality. Another limitation was the quality of the foF2 data reported by the 11 sites. The problems with part-time stations and poor observation quality mentioned in 2.1 suggest that the 11-station subset is not really an 11-station network. Since some stations, notably Vandenberg, produce more and better data, they have a greater influence on the calculated SSNis.

4.3 Geographic Coverage. Coverage of the 11-station network was another limitation. The eastern part of North America has more reporting sites (Cape Canaveral, Wallops Island, Goose Bay, Argentia, and Bermuda) than the western part (Vandenberg, College, and Resolute Bay). The only European site is Nicosia, which is closer to the Mideast. Taipei and Manila are the only Asian sites. The 11-station network, therefore, does not provide true global coverage. All these limitations must be kept in mind when interpreting the results.

5. RESULTS.

5.1 Mean, Median, and Standard Deviation. Table 3 gives the mean, median, and standard deviation of modeled-observed foF2 for all six of the stations studied. The Vandenberg storm distributions for both the global and subset case pass the skewness test for normal distributions. The quiet days distribution is skewed, but does center on the origin. The distributions for all days can be assumed to be normal. The Vandenberg distributions for quiet days and all days show a mean and median slightly greater than zero. A difference in accuracy of only 2 percent (calculated by taking the absolute value of the global - subset mean, divided by the larger of the two means times 100) exists between the global and subset groups. Sverdlovsk has distributions similar to Vandenberg's, but only the storm days distributions pass the skewness test. The difference between the subset group and the global group means is 12 percent for the worst case.

TABLE 3. (Modeled-Observed) foF2 (MHz) Distributions.

	Vandenberg	Sverdlovsk	Ashkhabad
QUIET DAYS			
Global Mean	0.02	0.15	-0.01
Subset Mean	0.02	0.14	-0.02
Global St Dev	1.20	1.10	0.98
Subset St Dev	1.20	1.20	1.00
Global Median	0.05	0.24	0.01
Subset Median	0.06	0.25	-0.03
STORM DAYS			
Global Mean	0.94	0.98	----
Subset Mean	0.92	1.10	----
Global St Dev	1.40	1.20	----
Subset St Dev	1.30	1.40	----
Global Median	0.89	0.93	----
Subset Median	0.87	1.00	----
ALL DAYS			
Global Mean	0.20	0.27	0.01
Subset Mean	0.20	0.28	0.01
Global St Dev	1.30	1.20	1.00
Subset St Dev	1.30	1.30	1.00
Global Median	0.18	0.34	0.02
Subset Median	0.20	0.37	-0.01

TABLE 3. (Modeled-Observed) foF2 (MHz) Distributions, Cont'd.

	Cape Canaveral	Slough	Magadan
QUIET DAYS			
Global Mean	-0.41	-0.31	-0.01
Subset Mean	-0.41	-0.37	-0.04
Global St Dev	0.99	0.87	1.10
Subset St Dev	0.94	1.00	1.10
Global Median	-0.36	-0.32	-0.07
Subset Median	-0.39	-0.39	-0.13
STORM DAYS			
Global Mean	0.50	0.69	0.81
Subset Mean	0.42	1.00	0.94
Global St Dev	1.70	1.30	1.10
Subset St Dev	1.50	1.60	1.20
Global Median	0.50	0.71	0.76
Subset Median	0.42	0.99	0.85
ALL DAYS			
Global Mean	-0.31	-0.21	0.12
Subset Mean	-0.32	-0.23	0.12
Global St Dev	1.12	0.97	1.12
Subset St Dev	1.05	1.16	1.20
Global Median	-0.31	-0.25	0.06
Subset Median	-0.33	-0.30	0.01

5.2 Modeled-Observed foF2 for Vandenberg and Sverdlovsk. Figures 1a and 1b show distributions of Modeled-Observed foF2 for Vandenberg and Sverdlovsk, respectively. Results from the control group (referred to from now on as the "global group") are at the top, and results from the test group (now called the "subset group") are at the bottom. The dark histograms show results for storm days; the lighter histograms, quiet days. The storm distributions are displaced to the right of the origin (X=0, Y=0), indicating that the modeled foF2s tend to be larger than the observed foF2s.

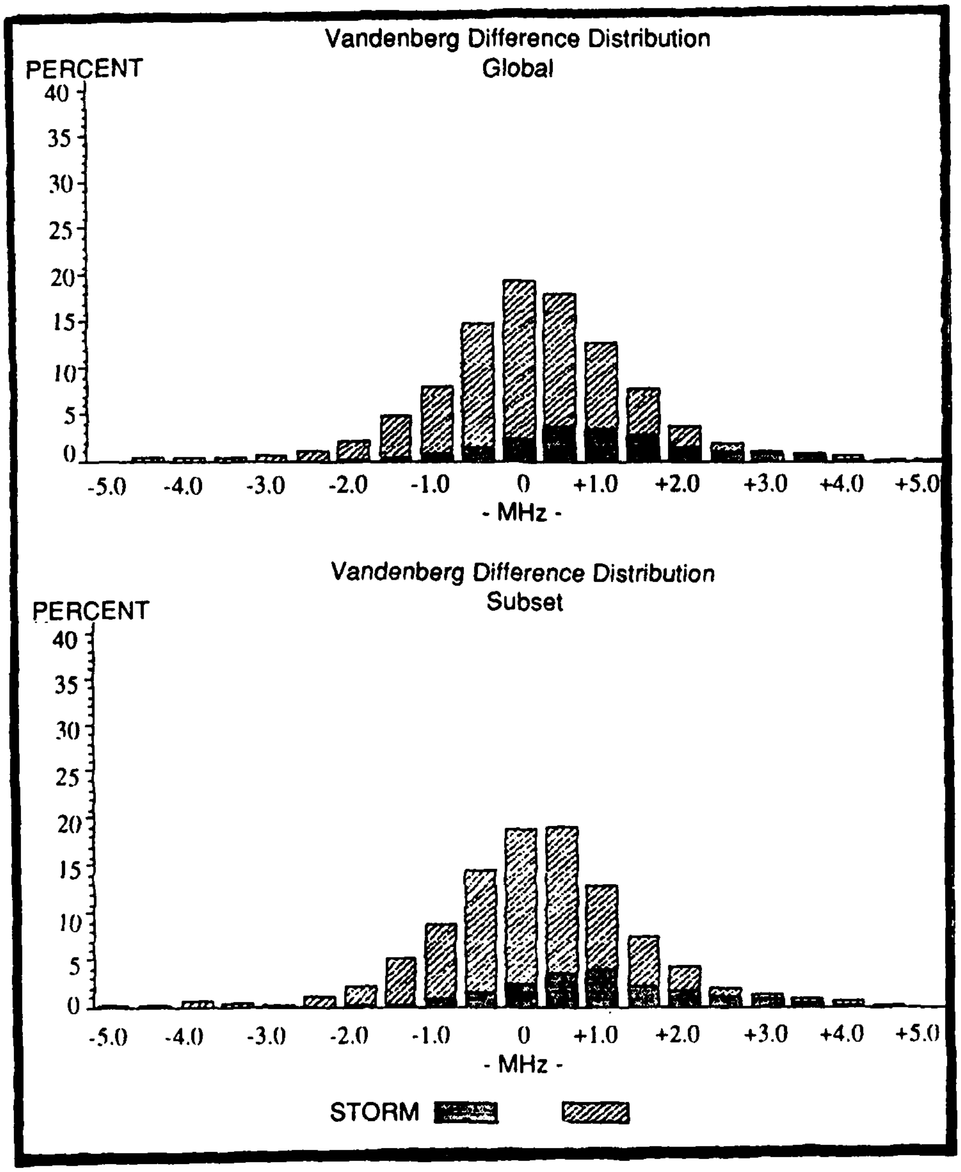

Figure 1a. Distributions of Modeled-Observed foF2 (MHz) for Vandenberg.

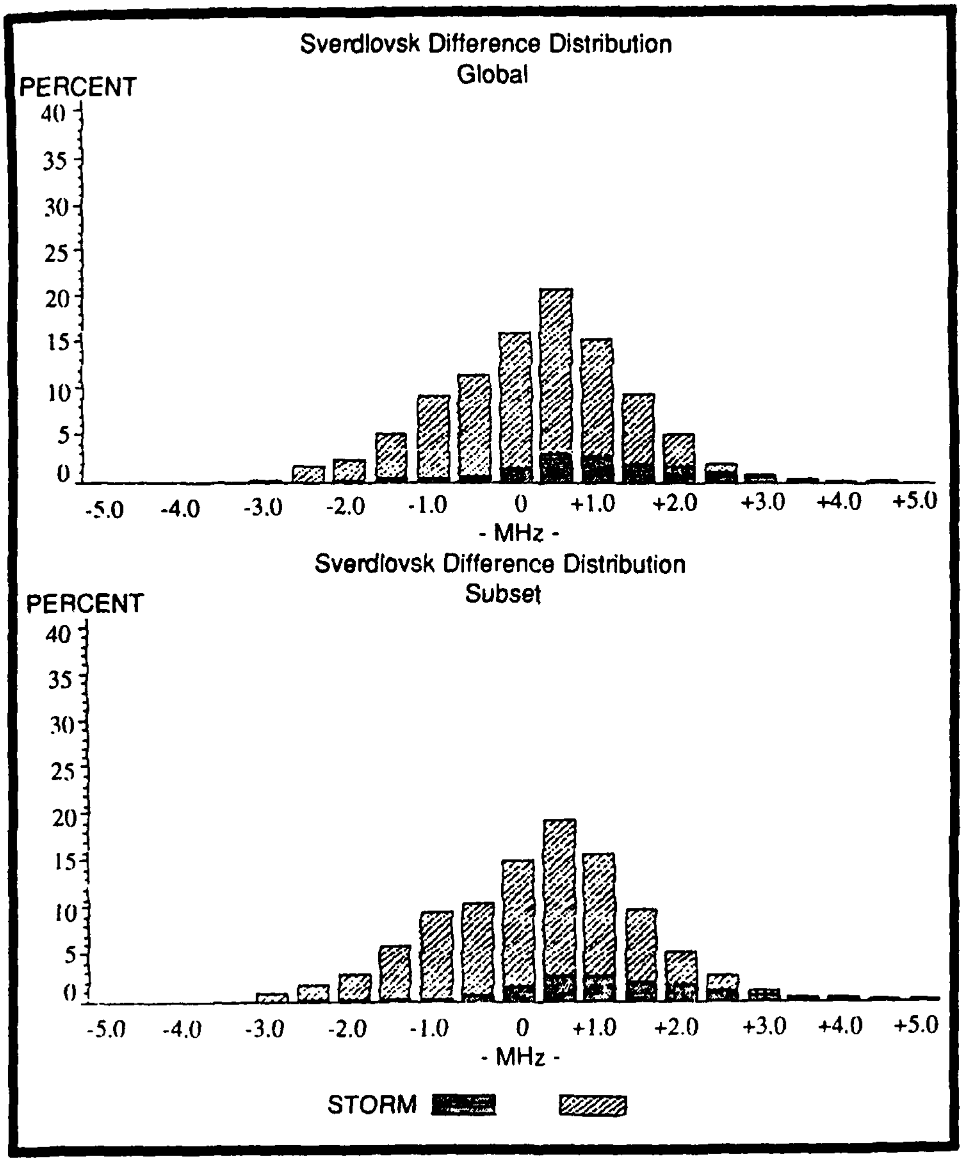

Figure 1b. Distributions of Modeled-Observed foF2 (MHz) for Sverdlovsk.

5.3 Modeled-Observed foF2 for Ashkabad and Cape Canaveral. Figures 2a and 2b show foF2 distributions for Ashkhabad and Cape Canaveral, respectively. See Table 3 for means, standard deviations, and medians. Because Ashkhabad has almost no storm days, those results are not included in the table. The quiet days and all days distributions are normal for the subset group, but not for the global group. The means for both groups are slightly less than zero. The worst case percent difference between the global and subset means seems large (50 percent), but it's due to the small values. Cape Canaveral has more storm days than Ashkhabad, but not nearly as many as Vandenberg. Cape Canaveral has a history of poor data quality (according to NGDC) and the results should be used with caution. The means and medians for both the global and subset groups are negative or close to zero, indicating that the model is under-predicting foF2s. The reason for this trend is not apparent. Only the subset distribution for the quiet days can be considered normal.

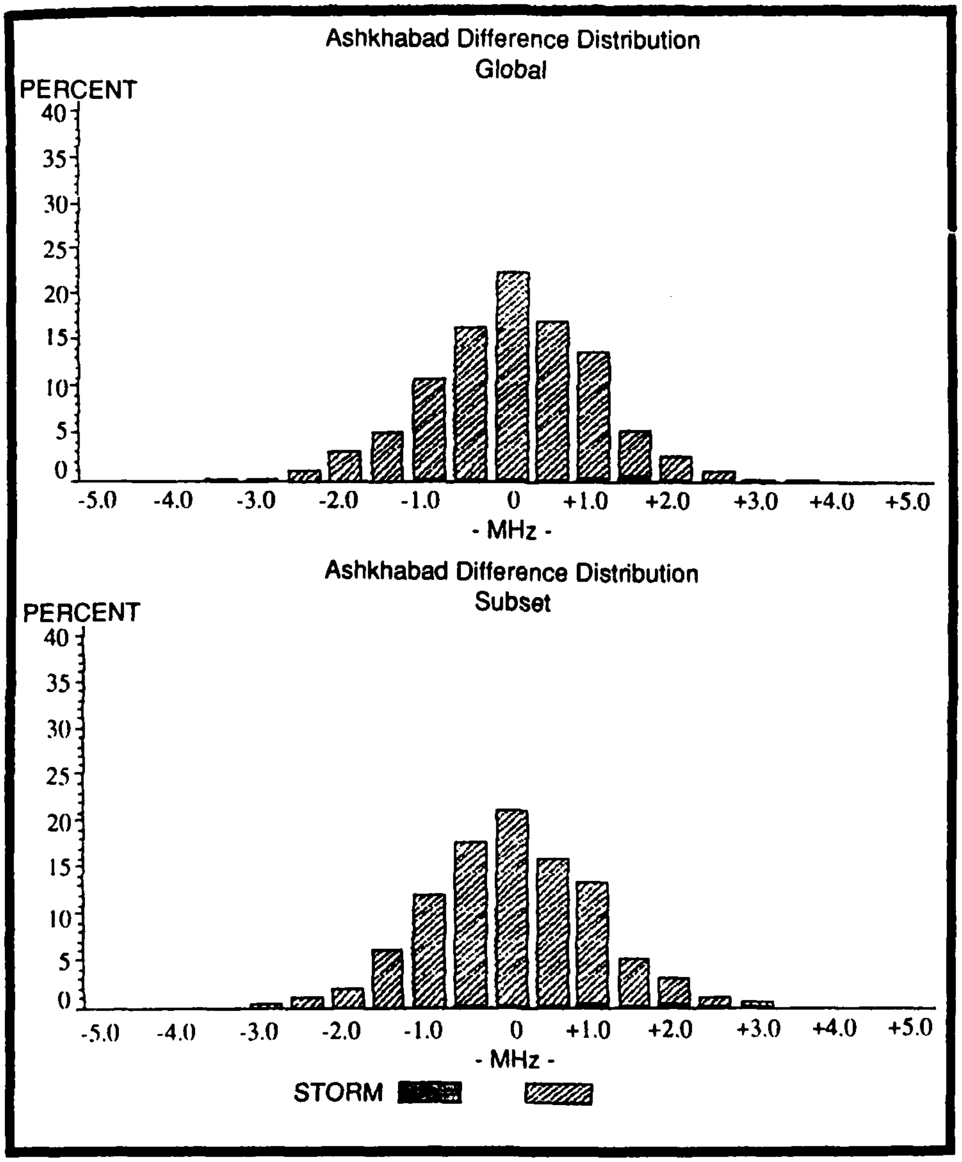

Figure 2a. Distributions of Modeled-Observed foF2 (MHz) for Ashkabad.

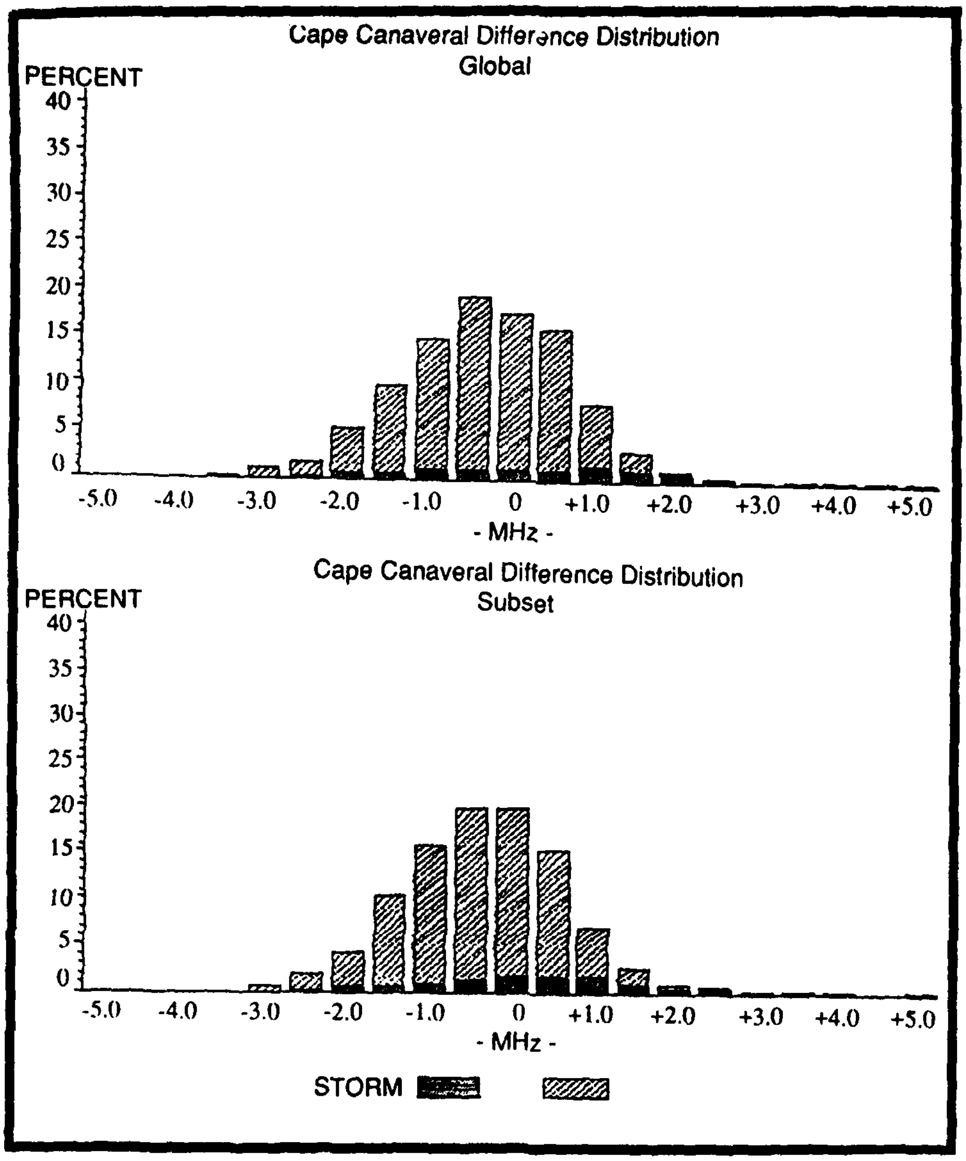

Figure 2b. Distributions of Modeled-Observed foF2 (MHz) for Cape Canaveral.

5.4 Modeled-Observed foF2 for Slough and Magadan. Figures 3a and 3b give foF2 distributions for Slough and Magadan, respectively; see Table 3 for means, medians, and standard deviations. Storm days and quiet days distributions for both the global and subset groups are normal. The storm distributions are displaced to the right of the origin (also shown by the positive mean and median), indicating that the model is again over-forecasting foF2. The observation count for storm days is still too small, with less than half the preferred count of at least 720 observations. Distributions for all days are skewed for both the global and subset groups. The model slightly under-predicts foF2 in both the quiet-days and all-days cases. The worst case difference between global and subset results for storm days, is 31 percent. This is the worst result of all the stations. The results for quiet days and all days are somewhat better, with a worst case difference of 16 percent. The lack of European sites in the subset network contributes to these poor results. Magadan has more storm days than Slough, and just over half the number of observations from Vandenberg. All distributions from Magadan are skewed. The largest difference between global and subset results occurs in the quiet days distributions, but the large difference (75 percent) is due to the fact that the means are very close to zero. The storm days case has a difference of 14 percent between the global and subset data.

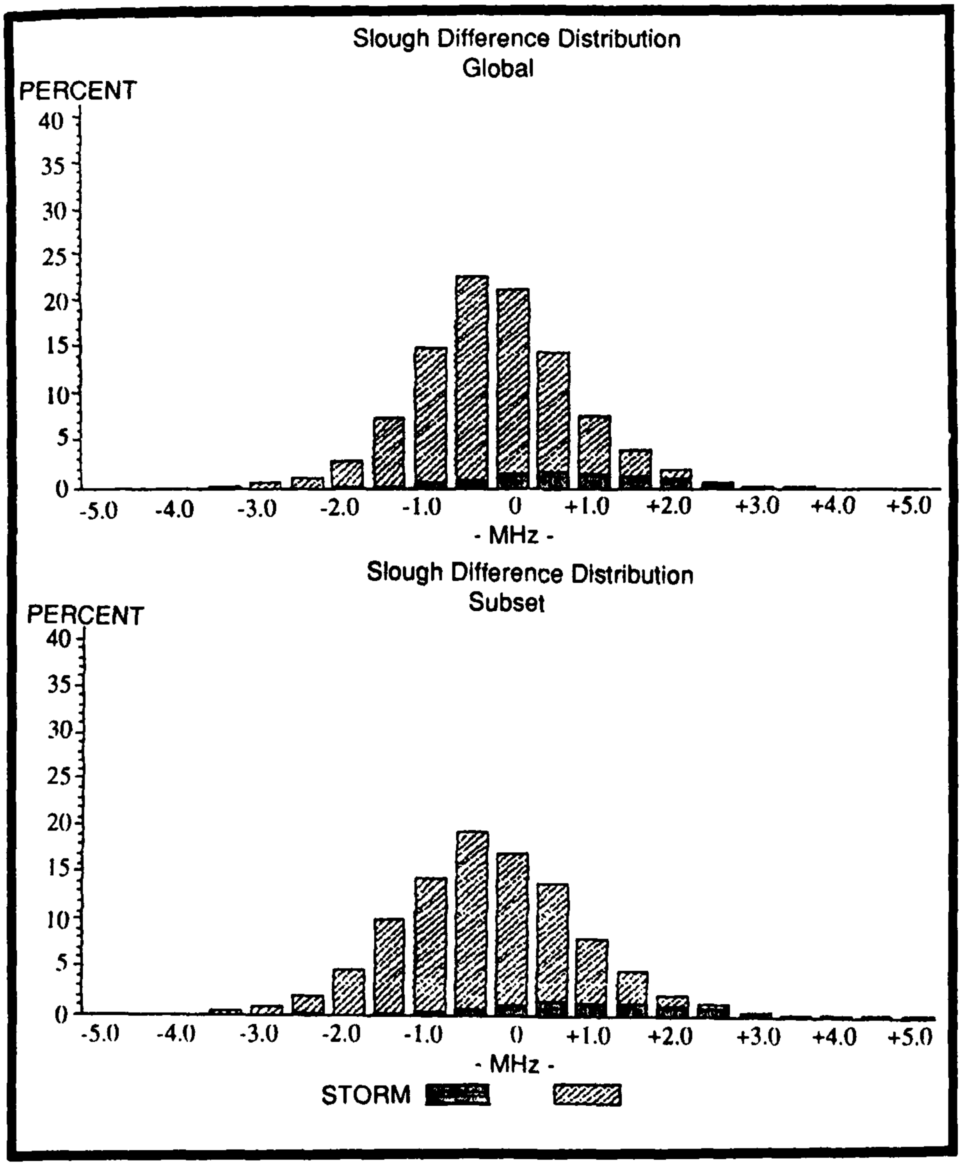

Figure 3a. Distributions of Modeled-Observed foF2 (MHz) for Slough.

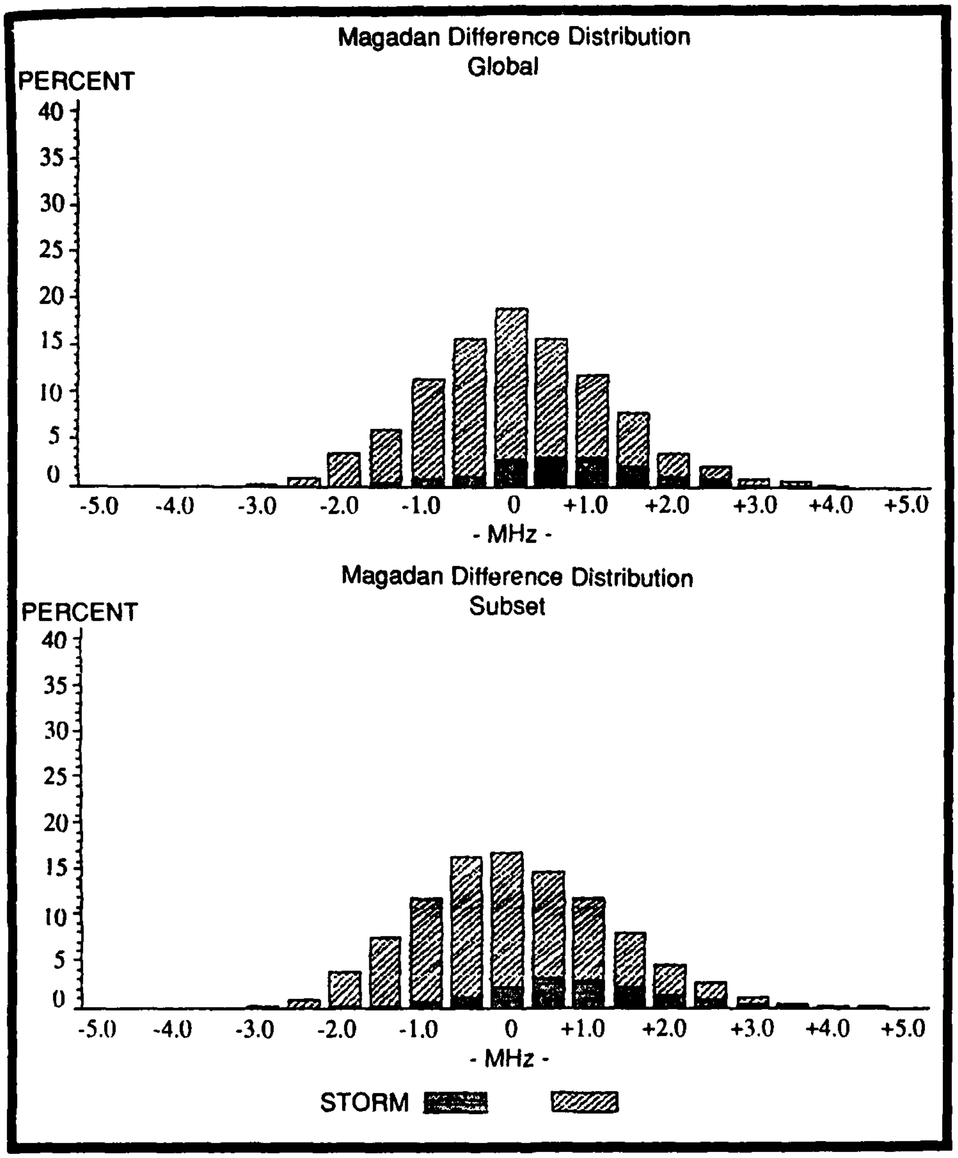

Figure 3b. Distributions of Modeled-Observed foF2 (MHz) for Magadan.

5.5 Summary of Distribution Results. The global and subset distributions for each of the six sites are very similar, indicating that the subset SSNis generally gave reasonable results. While the quiet days and all days distributions (in Table 1) look fairly close to normal, they are really skewed in half the cases, as the differences between mean and median values also show. When using the means and standard deviations of the differences between modeled and observed foF2 to judge the accuracy of the global and subset results, this fact must be kept in mind. The storm days distributions are not skewed, but they may not be truly normal either. The flattened shape of the distributions, with the larger number of values toward the extremes, has to be kept in mind when evaluating these distributions. Since Vandenberg has the largest number of storm days of the six sites, its results should be given the greatest consideration. Next, we look at the Vandenberg results in more detail, breaking down the distributions by Zulu hour.

5.6. Detailed Results for Vandenberg. Figures 4a (storm days) and 4b (quiet days) show Vandenberg's mean (x), standard deviation, and median (◊) of the difference between modeled and observed foF2 for each hour of the day. The plots for the global and subset data are very similar here, as well. For the storm days case, both global and subset plots show the distribution centered above the zero-error line (with means between 0.21 and 1.83 MHz), indicating that the model over-predicts foF2. This is true for all hours of the day, but is especially true for daylight hours (between 06 and 18 local, or 14 to 02Z). The daytime standard deviations are also larger than those at night, ranging from 0.70 to 1.71 MHz. There are also small-scale fluctuations that take place over a period of several hours, particularly during nighttime hours.

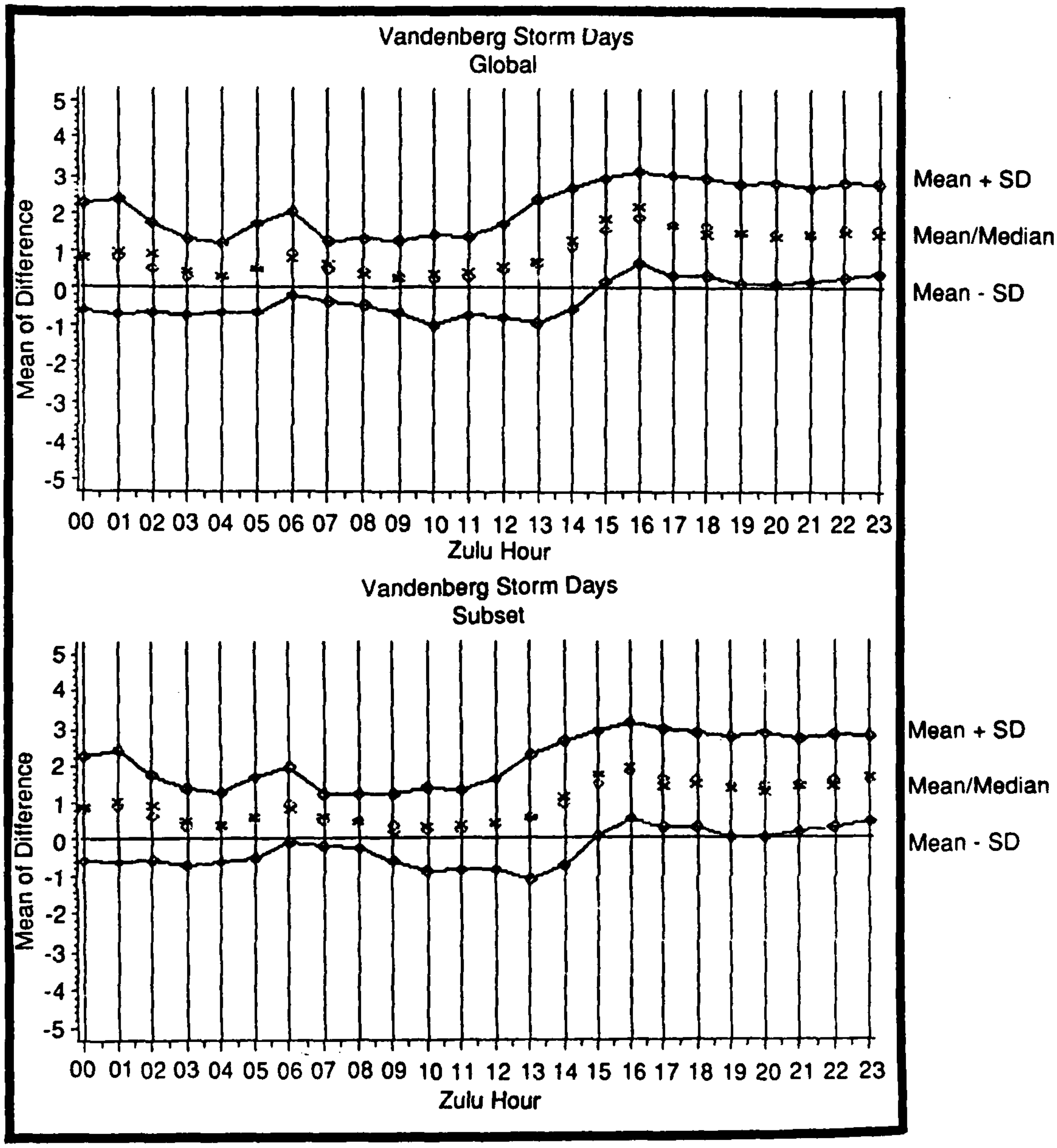

Figure 4a. Means (x), Medians (◊), and Standard Deviations of Distributions of Modeled-Observed Storm-Days foF2 (MHz) for Vandenberg by Zulu Hour.

Quiet day distributions are similar for global and subset data. These distributions are centered more closely on the zero-error line and show no diurnal variation. Here too, small-scale fluctuations with a period of several hours can be seen. The fluctuations are almost symmetric about the zero line; means range between -0.43 and 0.55 MHz. In this case, standard deviations show no diurnal change, ranging between 1.0 and 1.4 MHz.

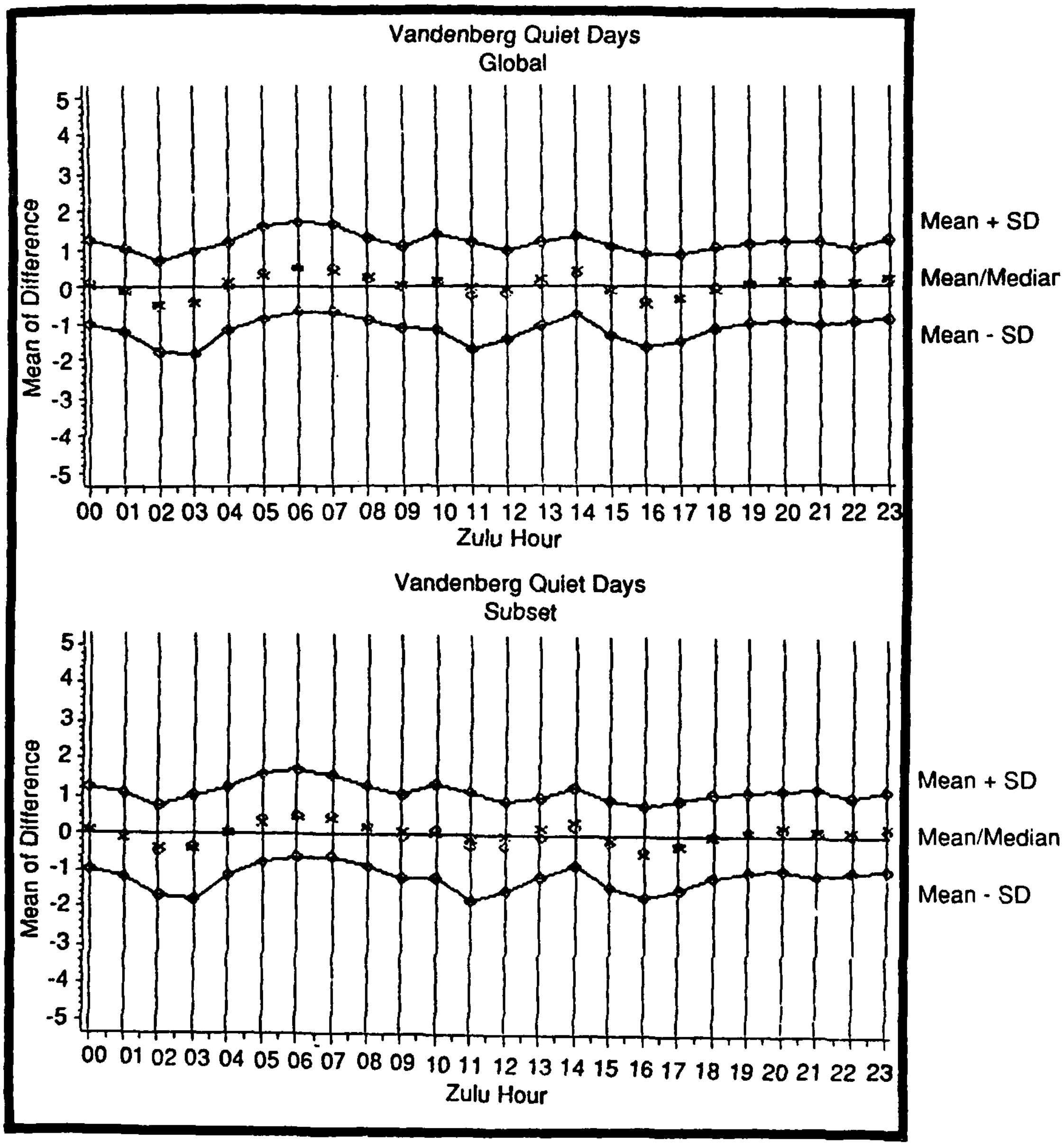

Figure 4b. Means (x), Medians (◊), and Standard Deviations of Distributions of Modeled-Observed Quiet-Days foF2 (MHz) for Vandenberg by Zulu Hour.

5.6.1 The model's overprediction of foF2 on storm days can be seen in Figures 5 and 6, which show hourly foF2 distributions for Vandenberg. Figures 5a, 5b, and 5c show observed foF2 for quiet days, storm days, and all days, respectively. Figures 6a amd 6b show modeled foF2 distributions for quiet days and storm days, respectively. The global, subset, and observed foF2s all show diurnal variation for the quiet days case, but observed foF2s on storm days show almost no diurnal variation--daytime values are almost the same as nighttime values. This is not the case in the model results, where diurnal variations in foF2 are a little more pronounced. The lack of a diurnal curve in observed foF2 should not be a surprise, given the methodolgy used to determine storm days with the QC program, which screens the daylight hours for foF2 values outside the range of expected values. The depletion of F-layer electrons by storm activity means that daytime foF2 values are lower than normal on storm days.

5.6.2 Global and subset modeled foF2 distributions are almost identical to each other for both quiet and storm days. The observed and modeled foF2 distributions also show the classic summertime pattern, with less diurnal variation in foF2 than in winter months. These distributions are evidence that the winter months were not well represented in the data sample, and that the results don't show how accurate the subset SSNis are then.

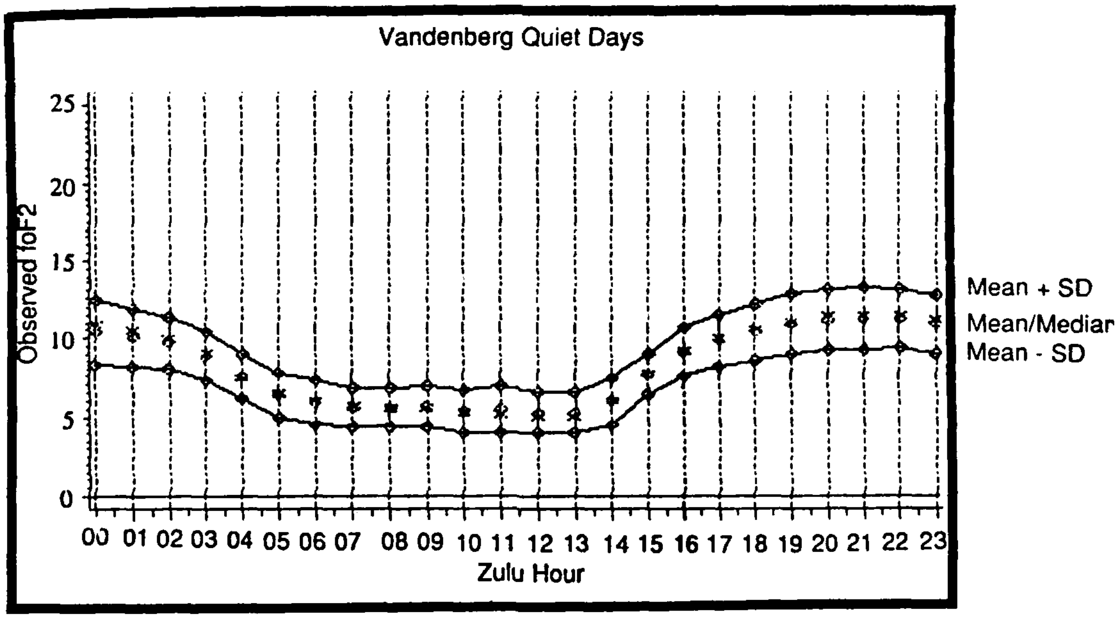

Figure 5a. Hourly Distributions of Observed foF2 (MHz) for Vandenberg, Quiet Days.

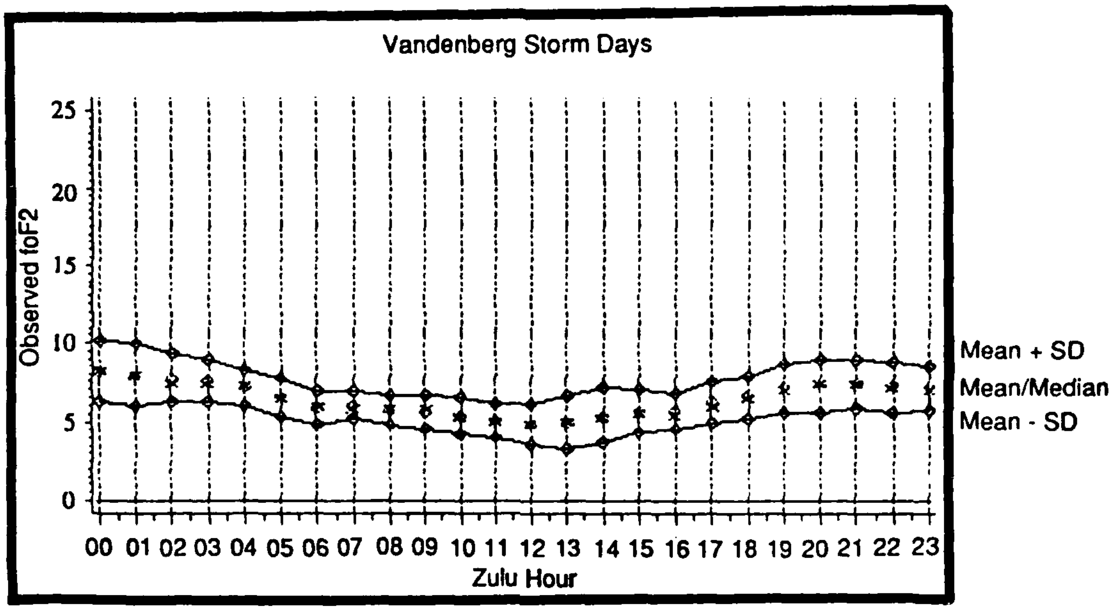

Figure 5b. Hourly Distributions of Observed foF2 (MHz) for Vandenberg, Storm Days.

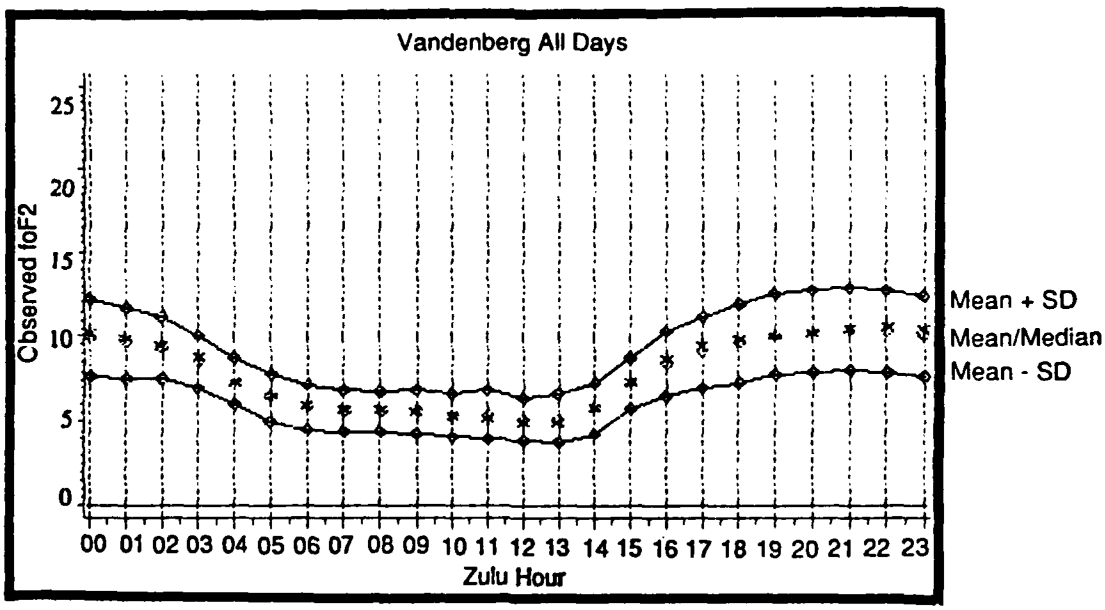

Figure 5c. Hourly Distributions of Observed foF2 (MHz) for Vandenberg, All Days.

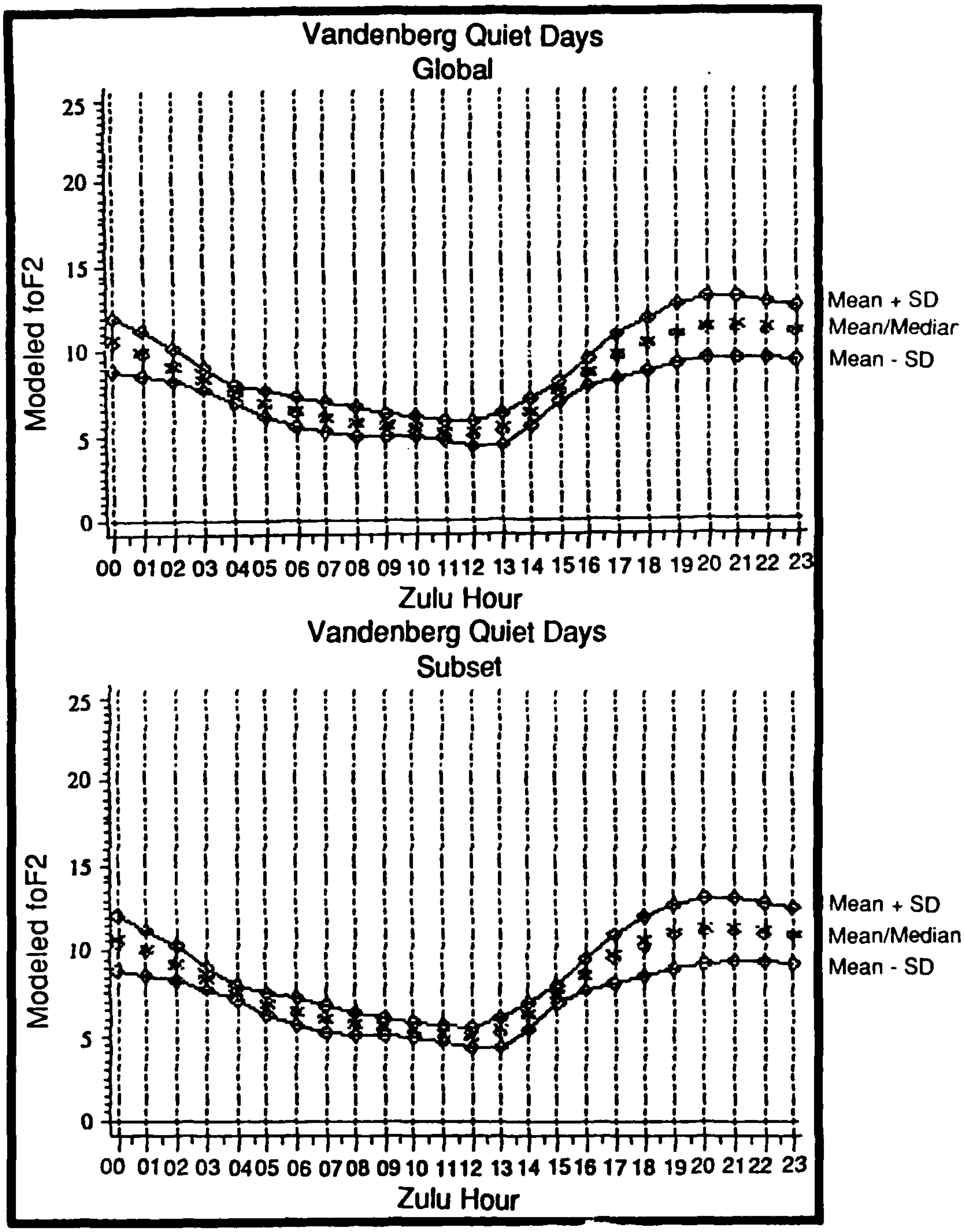

Figure 6a. Hourly Distributions of Modeled foF2 (MHz) for Vandenberg, Quiet Days.

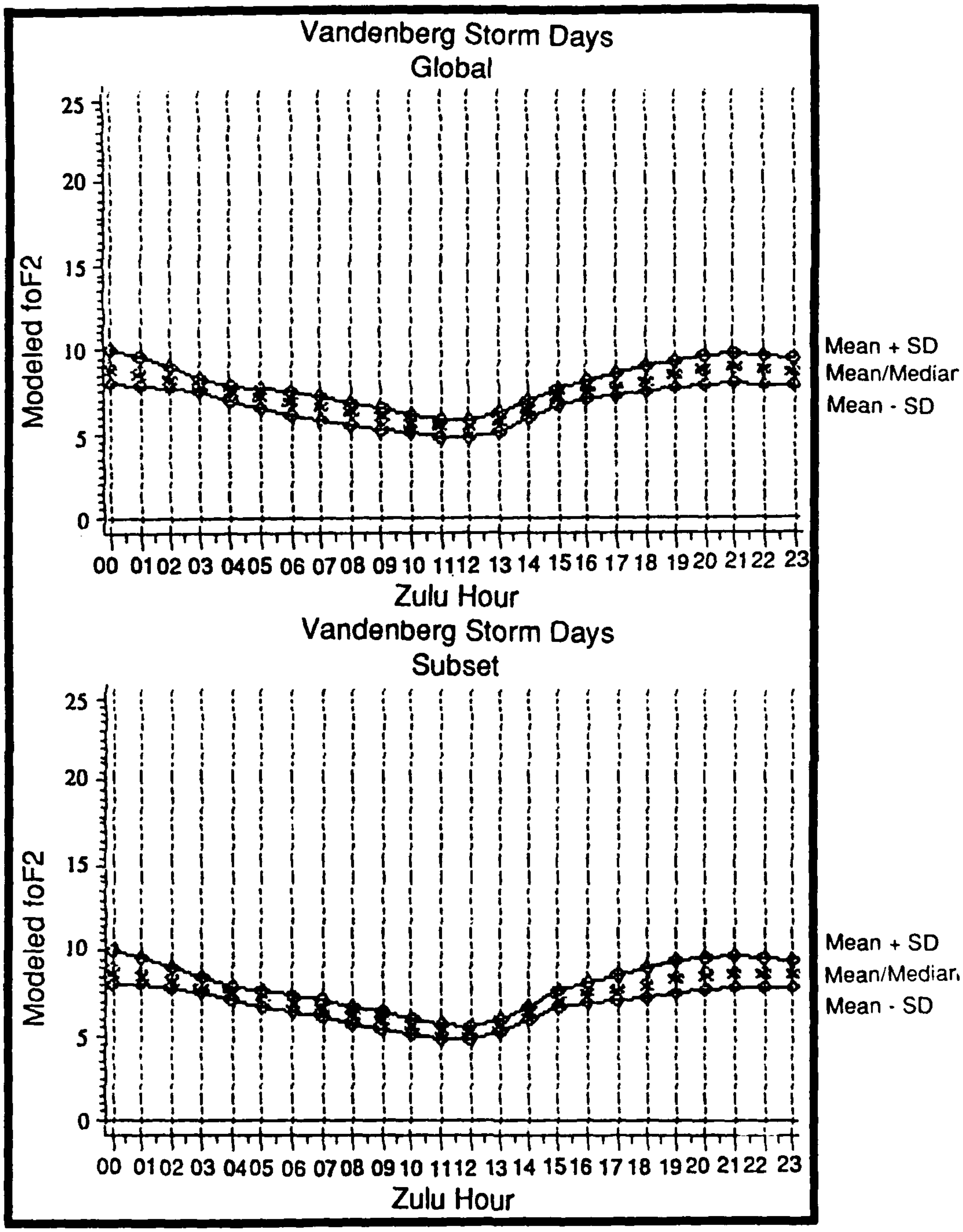

Figure 6b. Hourly Distributions of Modeled foF2 (MHz) for Vandenberg, Storm Days.

5.7 Correlations. Table 4 shows correlations between observed and modeled foF2 for all six sites. Figure 6 shows hourly correlations between observed and modeled foF2 for Vandenberg.

5.7.1 Both global and subset model runs produced foF2 values that correlated well with observed foF2s, as can be seen in Table 4. Correlations over the entire POR (for quiet and storm days) are between 0.84 and 0.92 for the global data, and between 0.80 and 0.91 in the subset case. Subset correlations are usually a little less than for the global data. In the cases of Vandenberg and Cape Canaveral, the subset correlations are the same or slightly higher. The Cape Canaveral results must be viewed with caution, however, since that station's observations, according to NGDC, can be unreliable.

TABLE 4. Correlations Between Modeled and Observed foF2.

	Global SSNIs			Subset SSNIs		
Station	*Quiet*	*Storm*	*All*	*Quiet*	*Storm*	*All*
Vandenberg	0.904	0.636	0.881	0.905	0.648	0.883
Sverlovsk	0.900	0.707	0.876	0.876	0.660	0.843
Ashkhabad	0.921	-----	0.918	0.918	-----	0.914
Cape Canaveral	0.897	0.236	0.862	0.909	0.308	0.881
Slough	0.935	0.754	0.912	0.895	0.654	0.854
Magadan	0.860	0.642	0.835	0.838	0.610	0.804

5.7.2 Correlations on storm days are always lower than on quiet days, sometimes considerably lower. The relatively small sample sizes on storm days limit the usefulness of those results. Figures 7a-c show hourly correlations for Vandenberg, the only station with a large enough sample size for hourly breakdowns. The correlations are lower during the nighttime hours for quiet days (7a), storm days (7b), and all days (7c). In the storm days case, the difference between the global and subset data is also greater during nighttime hours. In general, subset correlations are higher than global correlations during the early hours of the night, while global correlations are higher than subset correlations in the hours just before sunrise. Daytime correlations are virtually the same for both global and subset data. Global and subset correlations are also very similar for all hours in the quiet days (and therefore all days) cases.

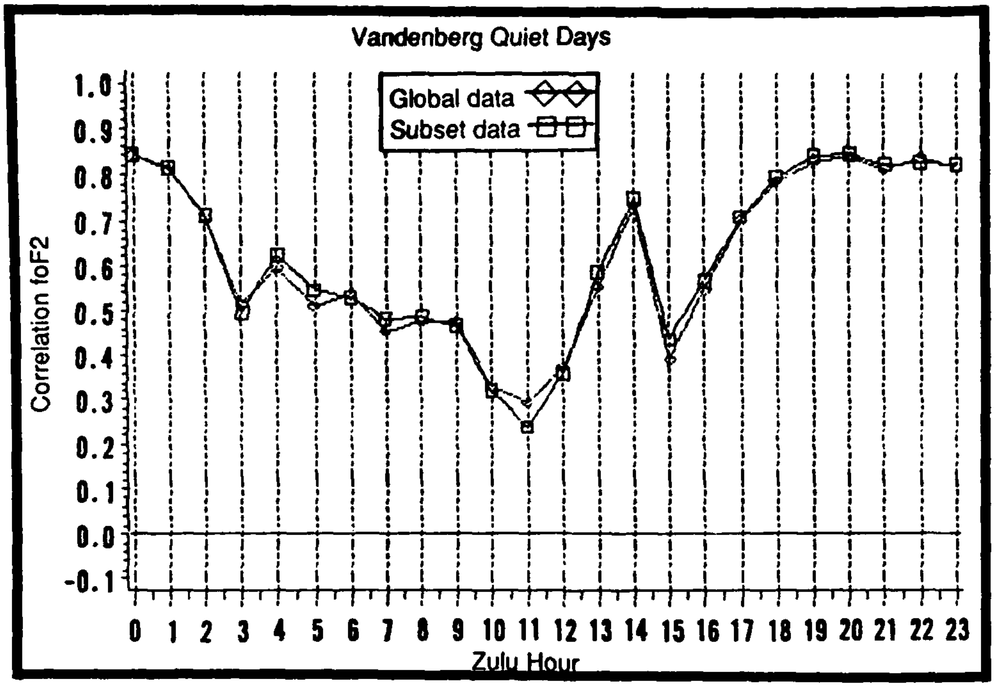

Figure 7a. Hourly Correlations Between Modeled and Observed foF2 (MHz) for Vandenberg, Quiet Days.

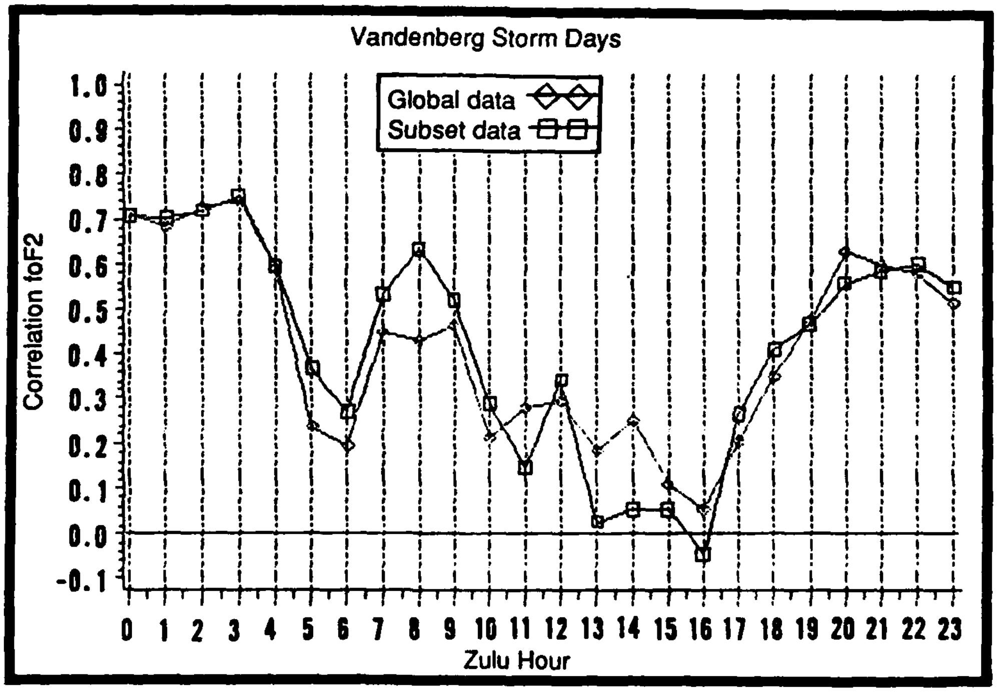

Figure 7b. Hourly Correlations Between Modeled and Observed foF2 (MHz) for Vandenberg, Storm Days.

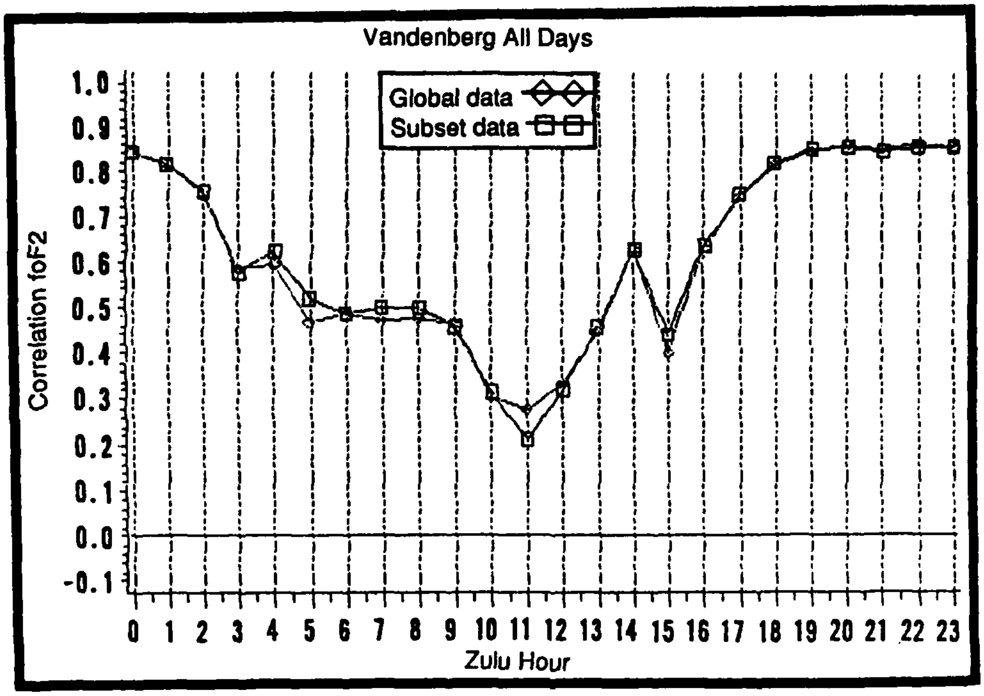

Figure 7c. Hourly Correlations Between Modeled and Observed foF2 (MHz) for Vandenberg, All Days.

5.8 RMS Error. Table 5 shows the six-station RMS errors (for the global and subset data), subdivided into columns for quiet days (left), storm days (middle), and all days (right) cases. The range of RMS errors for the six sites is small: between 0.99 and 1.9 MHz. All the sites except Vandenberg and Cape Canaveral show higher RMS errors in the subset data, but the difference in RMS between the global and subset data is always less than 1 MHz. In the case of Vandenberg, the differences between global and subset RMS is 0.02 MHz or less. The differences between global and subset data are larger in the case of Cape Canaveral, but the observations from this station are less reliable than those from Vandenberg. The largest difference between the global and subset data, for Slough, is still less than 0.5 MHz. None of the differences in RMS error are large enough to indicate a problem in the ICED model's accuracy, whichever type of SSNi is used as input.

TABLE 5. RMS Errors (MHz) for Modeled-Observed foF2.

	Global SSNis			Subset SSNis		
Station	*Quiet*	*Storm*	*All*	*Quiet*	*Storm*	*All*
Vandenberg	1.20	1.64	1.30	1.19	1.62	1.29
Sverdlovsk	1.11	1.56	1.19	1.20	1.79	1.30
Ashkhabad	0.99	---	1.01	1.00	----	1.03
Cape Canaveral	1.07	1.75	1.16	1.02	1.57	1.09
Slough	0.92	1.47	0.99	1.08	1.90	1.19
Magadan	1.07	1.38	1.13	1.13	1.54	1.21

5.9 RMS Errors--Vandenberg. The hourly RMS errors for Vandenberg are shown in Figure 8a (quiet days), 8b (storm days), and 8c (all days). Quiet days and all days plots show no diurnal variation in RMS errors, and the errors remain in a narrow range (1.0 to 1.5 MHz). There are some small-scale fluctuations in the RMS, but these don't appear to be tied to the diurnal cycle. The global and subset RMS errors are virtually identical. The storm days plot shows more of a diurnal variation in RMS, with errors increasing near sunrise and remaining relatively high during daylight hours. Errors range from about 0.8 MHz at night and 2.3 MHz during the day. This is expected, since the model is less accurate during daylight hours of storm days. There are also indications of smaller-scale fluctuations in RMS similar to quiet days and all days cases. The difference between the global and subset data is a little more pronounced than in the other two, but is still not significant. Of greater concern is the relatively high daytime RMS Error. A study using a more extensive POR would be needed to determine whether this problem is important enough to justify some sort of adjustment to the way the ICED model calculates foF2s for storm days.

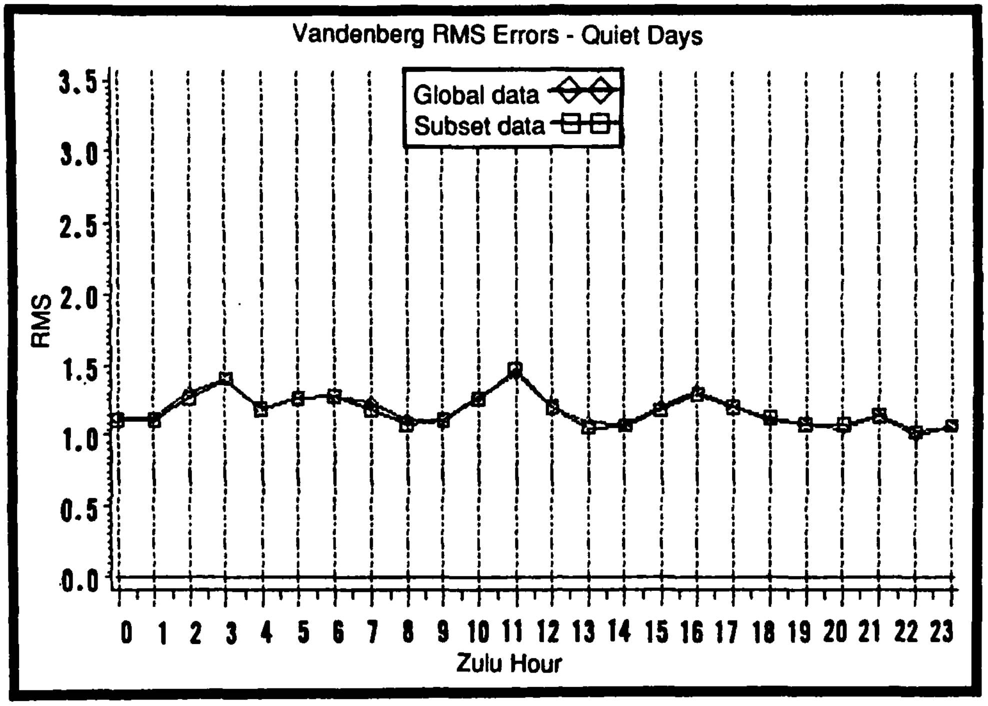

Figure 8a. ***Hourly RMS Errors for Modeled-Observed foF2 (MHz) for Vandenberg, Quiet Days.***

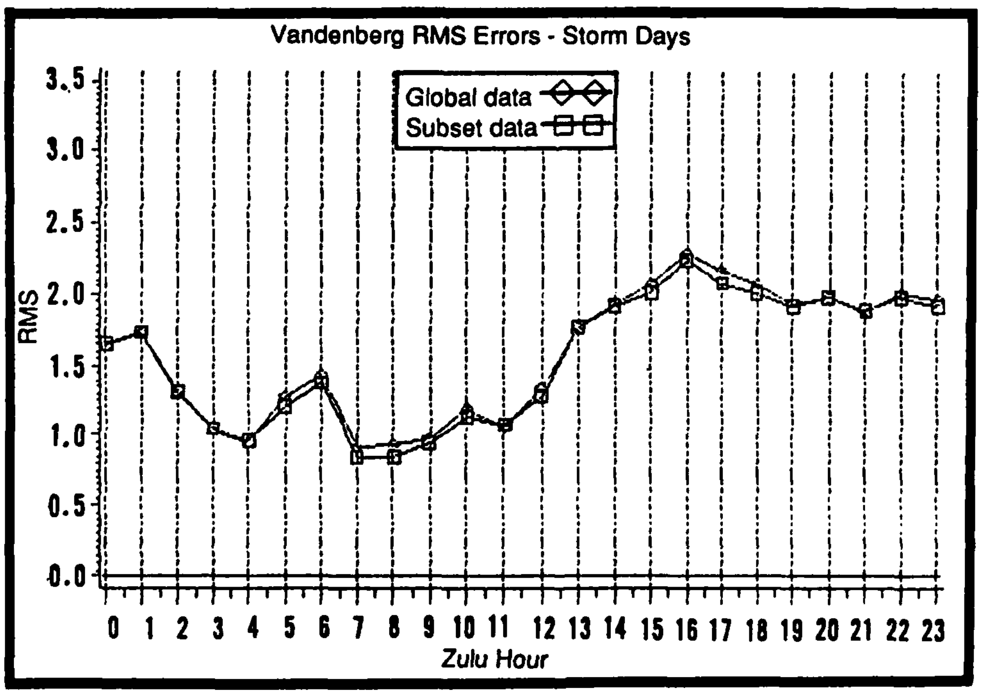

Figure 8b. ***Hourly RMS Errors for Modeled-Observed foF2 (MHz) for Vandenberg, Storm days.***

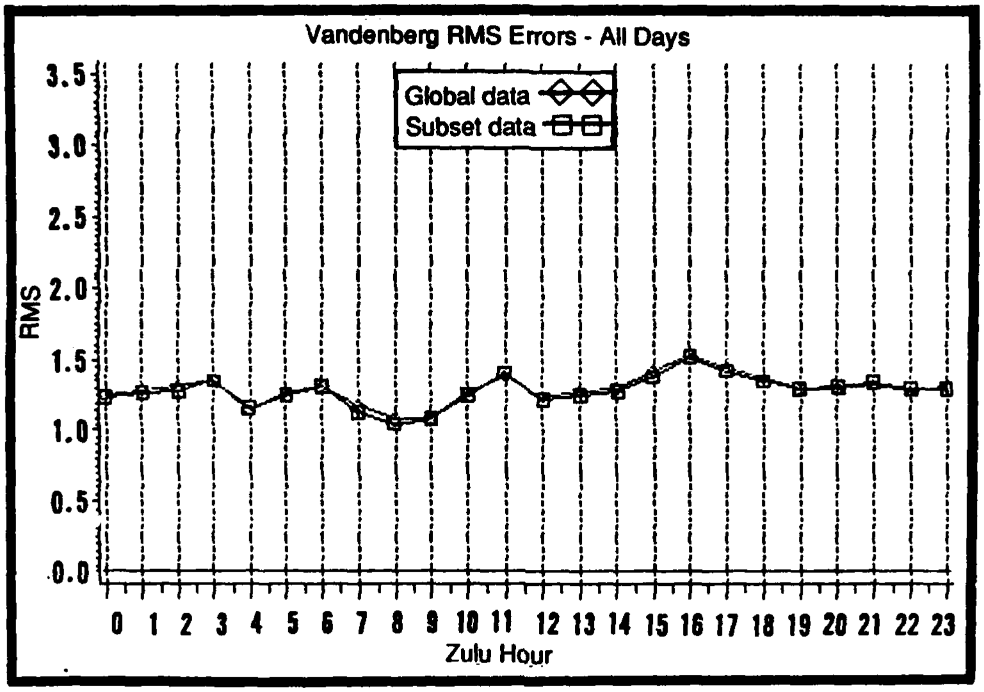

Figure 8c. Hourly RMS Errors for Modeled-Observed foF2 (MHz) for Vandenberg, All Days.

6. CONCLUSIONS.

6.1 Main Conclusion. We can conclude from this limited study that using foF2 data from the 11-station subset to calculate real time SSNis does not significantly reduce the accuracy of ICED output. That conclusion is supported by:

- similarities between global and subset SSNis for distributions in modeled-observed foF2.

- similarities between global and subset SSNis for hourly distributions in modeled-observed foF2 at Vandenberg.

- similarities in the correlations between observed and modeled foF2.

- similarities between RMS errors for global and subset SSNis.

The worst results in all the statistics were seen during storm days, but the limited amount of data makes it hard to draw any definite conclusions about those results.

6.2 Geographical Bias. The geographical bias toward North America in the 11-station ionosonde network explains why the results for Vandenberg and Cape Canaveral tended to be better than for the European and Soviet sites. Eleven sites may be enough to calculate reasonable global SSNis for use with ICED, but the ICED output for regions like Europe could be improved with a network that covers the globe more evenly.

6.3 Summary Conclusion. Increasing the number of digital ionosonde sites would have a limited effect on ICED output because of the limitations of an empirical model like ICED and the concept of an effective sunspot number as a way to initialize the model. The ICED model is not very responsive to changes in the the SSNi input. However, these results are not applicable to a physical model like the Parameterized Real-time Ionospheric Specification Model (PRISM), which initializes itself directly from data instead of from a proxy like SSNi. These results, in particular, cannot be used to draw conclusions about the necessary density of ionospheric sounding or sensing systems. We are confident of our results within the limitations discussed earlier.

SPECIALIZED TERMS AND ACRINABs

ACRINABs	acronym, initialisms, and abbreviations
AFGWC	Air Force Global Weather Central
AWS	Air Weather Service
DISS	Digital Ionospheric Sounding System
F2 layer	layer in the ionosphere at which electron density reaches its maximum
foF2	critical frequency of the F2 layer (highest electron density)
ICED	Ionospheric Conductivity and Electron Density Model
MHz	megahertz, a frequency measurement
NGDC	National Geophysical Data Center
POR	period of record
PRISM	Parameterized Real-time Ionospheric Specification Model
RMS error	root mean square error
Qe	equivalent Q index, calculated by AFGWC/WSE to measure size of auroral oval
QC	FORTRAN program that quality controls foF2 data
SESS	Space Environmental Support System
SCDB	SESS Climatic Database
SSNE	FORTAN program that calculates effective sunspot numbers
SSNi	Effective sunspot number for use with the ICED model
USAFETAC	USAF Environmental Technical Applications Center
WSE	AFGWC Space Environmental Support
Z	Zulu or Greenwich Mean Time

DISTRIBUTION

AWS/DO, Scott AFB, IL 62225-5008 2
AWS/XT, Scott AFB, IL 62225-5008 2
OL A, HQ AWS, Buckley ANG Base, Aurora, CO 80011-9599 1
SD/CWDA, PO Box 92960, Los Angeles, CA 90009-2960 1
OL-K, HQ AWS, NEXRAD Opnl Support Facility, 1200 Westheimer Dr. Norman, OK 73069 1
OL-L, HQ AWS, Keesler AFB, MS 39534-5000 1
OL-M, HQ AWS, McClellan AFB, CA 95652-5609 1
Det 1, HQ AWS, Pentagon, Washington, DC 20330-6560 3
Det 2, HQ AWS, Pentagon, Washington, DC 20330-5054 3
Det 3, HQ AWS, PO Box 3430, Onizuka AFB, CA 94088-3430 1
Det 9, HQ AWS, PO Box 12297, Las Vegas, NV 89112-0297 1
1WW/DN, Hickam AFB, HI 96853-5000 3
    11WS/DON, Elmendorf AFB, AK 99506-5000 1
    20WS/DON, APO San Francisco 96328-5000 1
    30WS/DON, APO San Francisco 96301-0420 1
2WW/DN, APO New York 09094-5000 3
    7WS/DON, APO New York 09403-5000 1
    28WS/DON, APO New York 09127-5000 1
    31WS/DON, APO New York 09136-5000 1
3WW/DN, Offutt AFB, NE 68113-5000 3
    9WS/DON, March AFB, CA 92518-5000 1
    24WS/DON, Randolph AFB, TX 78150-5000 1
    26WS/DON, Barksdale AFB, LA 71110-5002 1
4WW/DN, Peterson AFB, CO 80914-5000 3
    2WS/DON, Andrews AFB, MD 20334-5000 20
5WW/DN, Langley AFB, VA 23665-5000 3
    1WS/DON, MacDill AFB, FL 33608-5000 1
    3WS/DON, Shaw AFB, SC 29152-5000 1
    5WS/DON, Ft McPherson, GA 30330-5000 1
    25WS/DON, Bergstrom AFB, TX 78743-5000 1
AFGWC/SDSL, Offutt AFB, NE 68113-5000 3
AFGWC/WSE, Offutt AFB, NE 68113-5000 3
    OL B, AFGWC/R/E/SE2, 325 Broadway, Boulder, CO 80303-3328 1
    USAFETAC, Scott AFB, IL 62225-5438 6
7WW/DN, Scott AFB, IL 62225-5008 3
    6WS/DON, Hurlburt Field, FL 32544-5000 1
    15WS/DON, McGuire AFB, NJ 08641-5002 1
    17WS/DON, Travis AFB, CA 94535-5986 1
3350 TCHTG/TTGU-W, Stop 62, Chanute AFB, IL 61868-5000 2
3395 TCHTG/TTKO, Keesler AFB, MS 39534-5000 2
AFIT/CIR, Wright-Patterson AFB, OH 45433-6583 1
AFCSA/SAGW, Washington, DC 20330-5000 1
NAVOCEANCOMDET, Federal Building, Asheville, NC 28801-2723 1
NAVOCEANCOMDET, Patuxent River NAS, MD 20670-5103 1
NAVOCEANCOMFAC, Stennis Space Ctr, MS 39529-5002 1
NAVOCEANCOMFAC, NAS North Island, San Diego, CA 92135-5130 1
COMNAVOCEANCOM, Code N312, Stennis Space Ctr, MS 39529-5000 1
COMNAVOCEANCOM (Capt Brown, Code N332), Stennis Space Ctr, MS 39529-5001 1
Maury Oceanographic Library (NOC), Code XJL, Stennis Space Ctr, MS 39529-5001 1
FLENUMOCEANCEN, Monterey, CA 93943-5006 1

NOARL West, Monterey, CA 93943-5006 1
Naval Research Laboratory, Code 4323, Washington, DC 20375 1
Naval Postgraduate School, Chmn, Dept of Meteorology, Code 63, Monterey, CA 93943-5000 1
Naval Eastern Oceanography Ctr, U117 McCAdy Bldg, NAS Norfolk, Norfolk, VA 23511-5000 1
Naval Western Oceanography Ctr, Box 113, Attn: Tech Library, Pearl Harbor, HI 96860-5000 1
Naval Oceanography Command Ctr, COMNAVMAR Box 12, FPO San Francisco, CA 96630-5000 1
Pacific Missile Test Center, Geophysics Division, Code 3253, Pt Mugu, CA 93042-5000 1
Dept of Commerce/NOAA/MASC, Library MC5 (Jean Bankhead), 325 Broadway, Boulder, CO 80303 2
NOAA Library-EOC4WSC4, Attn: ACQ, 6009 Executive Blvd, Rockville, MD 20852 1
NOAA/NESDIS (Attn: Nancy Everson, E/RA22), World Weather Bldg, Rm 703, Washington, DC 20233 1
NOAA/NESDIS (Attn: Capt Taylor), FB #4, Rm 0308, Suitland, MD 20746 1
GL/LI, Hanscom AFB, MA 01731-5000 1
GL/LIM, Hanscom AFB, MA 01731-5000 1
GL/LIS, Hanscom AFB, MA 01731-5000 1
GL/LY, Hanscom AFB, MA 01731-5000 1
GL/PH, Hanscom AFB, MA 01731-5000 1
GL Library, Attn: SULLR, Stop 29, Hanscom AFB, MA 01731-5000 1
NGDC/WDC-A, 325 Broadway, Boulder, CO 80303 1
NGDC (E/GC2), 325 Broadway, Boulder, CO 80303 1
Space Environment Laboratory, 325 Broadway, Boulder, CO 80303 1
Space Environment Support Center, 325 Broadway, Boulder, CO 80303 1
Atmospheric Sciences Laboratory, Attn: SLCAS-AT-AB, Aberdeen Proving Grounds, MD 21005-5001 1
Atmospheric Sciences Laboratory, White Sands Missile Range, NM 88002-5501 1
U.S. Army Missile Command, ATTN: AMSMI-RD-TE-F, Redstone Arsenal, AL 35898-5250 1
Commander and Director, U.S. Army CEETL, Attn: GL-AE, Fort Belvoir, VA 22060-5546 1
Technical Library, Dugway Proving Ground, Dugway, UT 84022-5000 1
NWS W/OSD, Bldg SSM C-2 East-West Hwy, Silver Spring, MD 20910 1
NWS Training Center, 617 Hardesty, Kansas City, MO 64124 1
NCDC Library (D542X2), Federal Building, Asheville, NC 28801-2723 1
NIST Pubs Production, Rm A-405, Admin Bldg, Gaithersburg, MD 20899 1
DTIC-FDAC, Cameron Station, Alexandria, VA 22304-6145 2
AUL/LSE, Maxwell AFB, AL 36112-5564 1
AWSTL, Scott AFB, IL 62225-5438 35